AD-A054 257 CORNELL UNIV ITHACA N Y F/G 20/8
DYNAMICS OF THE CHEMISTRY OF ELECTRONICALLY EXCITED ATOMS IN DE--ETC(U)
MAY 78 J R WIESENFELD N00014-75-C-0828

UNCLASSIFIED NL

| OF |
AD
A054257

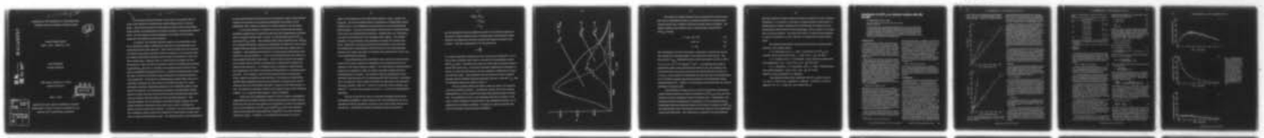

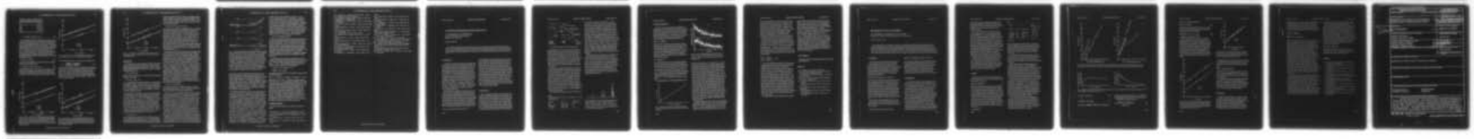

END
DATE
FILMED
6-78
DDC

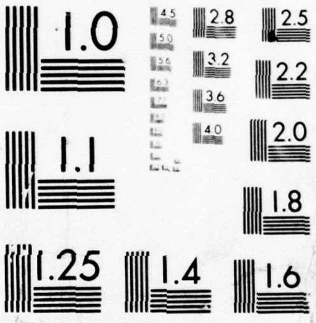

MICROCOPY RESOLUTION TEST CHART

NATIONAL BUREAU OF STANDARDS-1963-A

DYNAMICS OF THE CHEMISTRY OF ELECTRONICALLY EXCITED ATOMS IN DEFINED QUANTUM STATES

12

Annual Summary Report

April 1, 1977 - March 31, 1978

John Wiesenfeld
Cornell University

ONR Contract N00014-75-C-0828
Project NR 394-010

May 1, 1978

Approved for public release; distribution unlimited

Reproduction in whole or in part is permitted for any purpose of the United States Government

The research program described in this report is concerned with the study of the chemistry of electronically excited halogen atoms in the gas phase. These atomic species are interesting not only in terms of developing model systems for understanding the general chemistry of electronically excited atoms, but also because of their importance in the fields of laser isotope separation and chemical laser development.

In essence, this research concerns itself with the elucidation of the role of electronic energy in affecting the chemistry or photochemistry of excited halogen atoms and molecules. While much is known about the dynamics of chemical and physical processes which are carried out on the lowest potential energy hypersurface correlating with reactants and products in their electronic ground state, relatively little is known about the dynamics of such phenomena as energy transfer and chemical reactivity on higher-lying potential hypersurfaces. This may be compared to the present intense activity in the areas of vibrational photochemistry and i.r.-enhanced chemical kinetics where the effect of varying the internal energy distribution of molecular reagents is being determined. The chemistry of electronically excited states seems to be especially interesting not only because of the relatively large and, hence, presumably chemically significant,magnitude of the electronic quanta in many atoms and molecules, but also because generation of electronically excited species in states other than the ground state might reasonably be expected to open new reaction channels leading to novel chemical processes. Such chemical pathways can be examined in the light of orbital symmetry and state angular momentum conservation rules which can be used to elucidate the details of many excited state processes. In addition, the use of monochromatic laser irradiation makes possible the production of electronically excited molecules in highly defined quantum states. The temporal profile of the photoproducts of such monochromatic dissociations may be monitored in order to gain detailed insight into the nature of the potential hypersurfaces and regions of non-adiabaticity which control the behavior of excited species in the gas phase.

Our research program is centered on the use of time-resolved atomic absorption spectroscopy to monitor the production and disappearance of halogen atoms in defined quantum states, namely, the electronically excited $n^2P_{1/2}$ and ground $n^2P_{3/2}$ states. This technique offers great sensitivity and, because of its inherent selectivity, permits the experimenter to follow the course of even complex chemical reactions as both ground and excited state species may be monitored. Non-equilibrium distributions of electronically excited atoms were produced by pulsed photolysis. In one set of experiments this was carried out using standard white light flash lamps. Here the major goal was the acquisition of kinetic data to permit the determination of detailed rate constants for state-to-state processes. In a different type of experiment, atomic absorption spectroscopy was used in conjunction with photolysis by a tunable-pulsed dye laser. This technique, laser induced photodissociation spectroscopy (LIPS), permits the detection of product atoms in the ground or electronically excited states immediately following the production of electronically excited molecules above the dissociation threshold. Analysis of this data permits, in turn, the analysis of molecular spectra in the continuum region where classical methods, e.g., rotational band analysis, cannot be applied.

There has been considerable progress in both the areas of quantitative photochemistry and reaction kinetics involving electronically excited species. During the past year we have carried out an experiment in which the branching ratio for the production of $Br(4^2P_{1/2})$ and $Br(4^2P_{3/2})$ atoms was monitored following the broad band white light flash photolysis of the alkyl bromides, CH_3Br and C_2H_5Br. In addition, we monitored the production of bromine atoms in the photolysis of the perfluorinated halides, CF_3Br, C_2F_5Br, and n-C_3F_7Br. We have ascertained that the production of electronically excited bromine atoms is very inefficient for the photolysis of the perhydrogenated alkyl bromides. The yield of electronically excited atoms is somewhat higher in the case of the perfluorinated molecules, although these are considerably less than for the photolysis of the analogous alkyl iodides. The photodissociation of CF_3Br resulted in the production of roughly 66% excited state atoms, while that of n-C_3F_7Br resulted in the production of less than 10%. The deactivation of electronically excited bromine by the perhydrogenated bromides was roughly two orders of magnitude more efficient than for the case of the perfluorinated molecules.

These observations were considered in the context of an earlier theory which was devised to explain the dependence of the branching ratio on the structure of the source molecules studied. The lower yields of excited bromine atoms may be explained in terms of smaller spin-orbit coupling and lower electronegativity of bromine. The relatively efficient deactivation of electronically excited bromine by the perhydrogenated alkyl bromides is presumably due to the relatively close resonance between the magnitude of the electronic quantum in bromine, 3686 cm^{-1}, and the C-H stretch in alkyl bromides, ca. 3000 cm^{-1}. No such close resonance occurs in the case of the perfluorinated molecules.

The use of LIPS for the study of continuous absorption above photodissociation thresholds in small molecules has been demonstrated by our investigation of the Br_2 absorption spectrum in the visible region between 400 and 500 nm. The spectrum contains contributions from the transitions

$$X^1\Sigma_g^+ \rightarrow A^3\pi_{1u}$$
$$\rightarrow B^3\pi_{0^+u}$$
$$\rightarrow {}^1\pi_{1u} \quad .$$

Br_2 was photolyzed using our tunable dye laser in the continuum region and the relative yields of ground state and electronically excited bromine atoms following the photolysis pulse was measured with atomic absorption spectroscopy. From this measurement of the branching ratio

$$\Phi = \frac{Br^*}{Br} \quad ,$$

the relative extinction coefficient for the B state may be determined, as it is only B state absorption which leads to production of electronically excited $Br(4^2P_{1/2})$ atoms. Absorption into either one of the other two states produces ground state atoms only. As the total extinction coefficient for absorption is known, one may then calculate the absolute extinction coefficient for absorption into the B state. This absorption data may then be fit with a modified gaussian and the residuals represent absorption into the A state and ${}^1\pi_{1u}$ state. The absorption spectra are shown in Figure 1.

We are currently refining this data in order to improve the resolution of the Br_2 absorption spectrum. Of particular concern will be the accurate determination of a curve of growth for ground state bromine atoms in absorption. The appearance of the A state absorption near 500 nm should, on the basis of other information concerning the A state absorption spectrum, be an artifact due to our fitting procedure. We hope to be able to reconcile this with the classically derived spectral information.

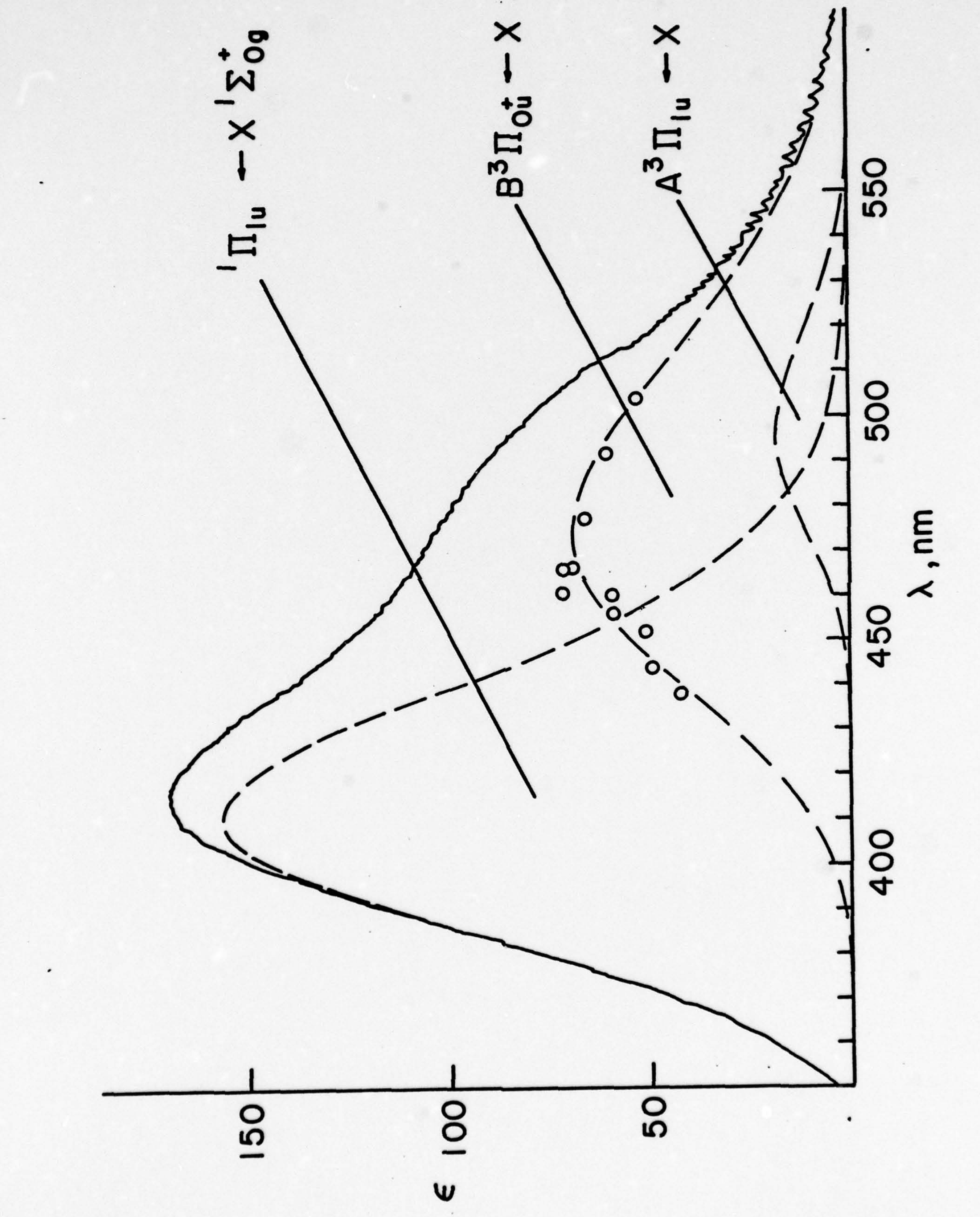
$^1\Pi_{1u} \leftarrow X\,^1\Sigma^+_{0g}$
$B^3\Pi^+_{0u} \leftarrow X$
$A^3\Pi_{1u} \leftarrow X$
ε
150
100
50
400
450
500
550
λ, nm

The studies of reaction kinetics have also borne fruit in that we have been able to demonstrate directly the chemical production of electronically excited species from a reaction involving low-lying states of reagents. The subject reaction being studied is that of electronically excited iodine $I(5^2P_{1/2})$ with Br_2

$$I^* + Br_2 \rightarrow IBr + Br^* \qquad [1a]$$

$$\rightarrow IBr + Br \qquad [1b]$$

$$\rightarrow I + Br_2 \qquad [2].$$

This investigation has taken advantage of our ability to monitor both ground and excited state temporal profiles of the iodine and bromine atoms. The rate constant, k_{Br_2}, characterizing the overall deactivation process at 295° K is $5.6 \pm 0.2 \times 10^{-11}$ cm^3 $molecule^{-1}$ sec^{-1}. By monitoring the growth of *ground state iodine atoms following deactivation by* Br_2 *and comparing this* to that observed in the known quenching (no chemical reaction possible) of I^* by H_2, it was possible to demonstrate that less than 10% of the deactivation of I^* by bromine proceeds <u>via</u> physical quenching and concommitant energy transfer (reaction [2]). Rather, the deactivation must proceed with the chemical production of bromine atoms.

The production of bromine atoms in both the ground and electronically excited states following the reactive deactivation of $I(5^2P_{1/2})$ by Br_2 was also monitored using the appropriate bromine resonance lines. Observation of the absorption transient corresponding to attenuation of the resonance emission demonstrates that the predominant product of the reactive collision is $Br(4^2P_{1/2})$ with approximately 80% of the bromine atoms being formed in the electronically excited spin-orbit state. This observation is consistent with the prediction that total electronic angular momentum should be conserved in such a reaction. Furthermore, it is possible on the basis of simple molecular orbital theory to predict that the reaction coordinate for the abstraction of a bromine atom by electronically excited iodine should proceed via a side-on attack of the iodine atom on the Br_2 molecule. The simple MO theory is currently being expanded to include consideration of other reactions of electronically excited halogen atoms.

The following publications were generated during the contract period covered by this summary report:

J. R. Wiesenfeld and G. L. Wolk, "Deactivation of $I(5^2P_{1/2})$ by chemical reaction with HBr and DBr," J. Chem. Phys., 67, 509 (1977).

T. G. Lindeman and J. R. Wiesenfeld, "Laser Induced Photodissociation Spectroscopy: Br_2," Chem. Phys. Lett., 50, 364 (1977).

W. L. Ebenstein, J. R. Wiesenfeld, and G. L. Wolk, "Photodissociation of Alkyl Bromides," Chem. Phys. Lett., 53, 185 (1978).

Reprints of these publications are attached.

Two graduate students were associated with this research program: Mr. Gary L. Wolk and Mr. Theodore G. Lindeman. In addition, an undergraduate, Mr. W. L. Ebenstein, also worked with us.

Deactivation of I($5^2P_{1/2}$) by chemical reaction with HBr and DBr

J. R. Wiesenfeld[a] and G. L. Wolk

Department of Chemistry, Cornell University, Ithaca, New York, 14853

(Received 17 March 1977)

The collisional deactivation of electronically excited iodine atoms, I($^5P_{1/2}$), by CH_4, C_3H_8, HBr, and DBr has been investigated using time-resolved atomic resonance spectroscopy. This technique permits direct determination of the yield of I($5^2P_{3/2}$) following the deactivation of the excited atoms by the added gas. The experiment demonstrated that the deactivation of I($5^2P_{1/2}$) by CH_4 and C_3H_8 proceeds by physical quenching, but deactivation by HBr and DBr occurs *via* metathetical chemical reaction to form HI + Br($4^2P_{3/2}$). This nonadiabatic reaction is discussed in the context of a curve-crossing model involving vibrationally excited virtual states of the deactivating molecule.

INTRODUCTION

Investigations of the collisional deactivation of electronically excited halogen atoms have played a significant role in the elucidation of those chemical and physical processes which govern the behavior of electronically excited species in the gas phase. Thus, the overall rate coefficients for deactivation of X($n^2P_{1/2}$), where X = Cl, Br, or I have been measured[1–9] using a variety of techniques, the difficulty of making such determinations being I < Br < Cl.

While such a broad collection of data has been useful to the development of a theoretical description of the deactivation of electronically excited halogens, it would appear that a complete understanding of these phenomena must await the analysis of the products of the collisional events. Discrimination between physical energy transfer (with concomitant excitation of internal modes of the quenching molecule and relative translation between products) and actual metathetical chemical reactions resulting in the formation of new molecular products would thus be possible. Recent developments in excited halogen chemistry have included the observation of infrared emission from vibrationally excited hydrogen halides[3,4,7,8,10] produced following electronic–vibrational (E–V) energy transfer

$$X(n^2P_{1/2}) + HY \rightarrow X(n^2P_{3/2}) + HY^{\dagger}$$

where X = Br, or I and Y = F, Cl, or Br. These E–V processes have been interpreted in terms of coupling via long-range interactions,[11] a process which is greatly facilitated by resonance between the magnitudes of the electronic and vibrational quanta involved.[12,13] Measurements of overall deactivation efficiencies for spin–orbit relaxation of excited halogens by hydrogen halides and hydrogen isotopes also appear to indicate that such long-range quadrupole–multipole interactions play a significant role, but theory and experiment do not yet appear to be in full agreement with respect to the relative importance of E–V processes as compared to translational excitation (E–T) of the product species.[9,14,15]

Direct evidence for chemical reaction as an efficient route for the collisional deactivation of I($5^2P_{1/2}$) by halogen molecules[16] and nitrosyl halides[7] has been obtained using kinetic spectroscopy. In addition, I-atom abstraction may play a minor role in the deactivation of I($5^2P_{1/2}$) by alkyl iodides[18–20] as does H-atom abstraction to form HI in the deactivation of excited iodine atoms by ethane and propane.[21] The deactivation of Br($4^2P_{1/2}$) by HI, which may proceed via thermally accessible adiabatic and nonadiabatic reactive channels to produce HBr + I($5^2P_{1/2}$) or HBr + I($5^2P_{3/2}$) respectively, has been demonstrated[7] to undergo quenching with formation of Br($4^2P_{3/2}$) + HI. However, Pritt and Coombe[8] has suggested that the anomalously rapid deactivation of I($5^2P_{1/2}$) by HBr and HI may be the consequence of nonadiabatic reactions, e.g.,

$$I(5^2P_{1/2}) + HBr \rightarrow Br(4^2P_{3/2}) + HI. \tag{1}$$

This would be at variance with the view of Bergman *et al.*,[7] who invoked a simple valence-bond model to explain the relative stability of Br($4^2P_{1/2}$) [with respect to Br($4^2P_{3/2}$)] upon collision with HI. The experiments described below test this model and permit its further refinement.

EXPERIMENTAL

The apparatus utilized in these experiments has been described previously.[22,23] n-C_3F_7I was used as the source for iodine atoms. A dilute solution (typically $5–50 \times 10^{-3}$ torr) of n-C_3F_7I in an argon buffer ($p_{\text{total}} = 60$ torr) was exposed to a pulse of light ($t_{1/2} \approx 10$ μsec, $E = 100$ J). Thermalization of species in the quartz reaction vessel was insured by the presence of the argon buffer gas. The temporal profiles of $[I^*]_t$ [$I^* \equiv I(5^2P_{1/2})$] or $[I]_t$ [$I \equiv I(5^2P_{3/2})$] following the flash were monitored by observing the attenuation of atomic resonance radiation at 178.3 nm ($6^2P_{3/2} - 5^2P_{3/2}$) or 206.2 nm ($6^2P_{3/2} - 5^2P_{1/2}$). The resonance transitions were excited in a microwave powered electrodeless discharge lamp. The lamp contained a small amount of solid I_2 with 1 torr of argon. The vapor pressure of I_2 in the lamp was controlled by varying the temperature of a cold finger, typically in the range 263–265 °K. The transient absorption signal was monitored by using a solar-blind HTV-R116 photomultiplier tube and digitized with a Biomation 802 Transient Recorder. The photomultiplier gain was decreased during the photolytic flash by switching dynodes 5 and 7 to a common voltage. This minimized the magnitude of the scattered light pulse reaching the digitizing electronics and permitted accurate absorption measure-

---

[a] Camille and Henry Dreyfus Teacher–Scholar.

ments within 25 μsec following the initiation of photolysis. Typically 8–16 runs were averaged in order to enhance the signal. Gases in the reaction vessel were swept out between individual kinetic runs. The photolysis of HBr or DBr was prevented[24] by the introduction of CCl_4 into a 1-cm thick annular filter chamber around the quartz reaction vessel. No decomposition of the CCl_4 was noted during the course of an experimental session.

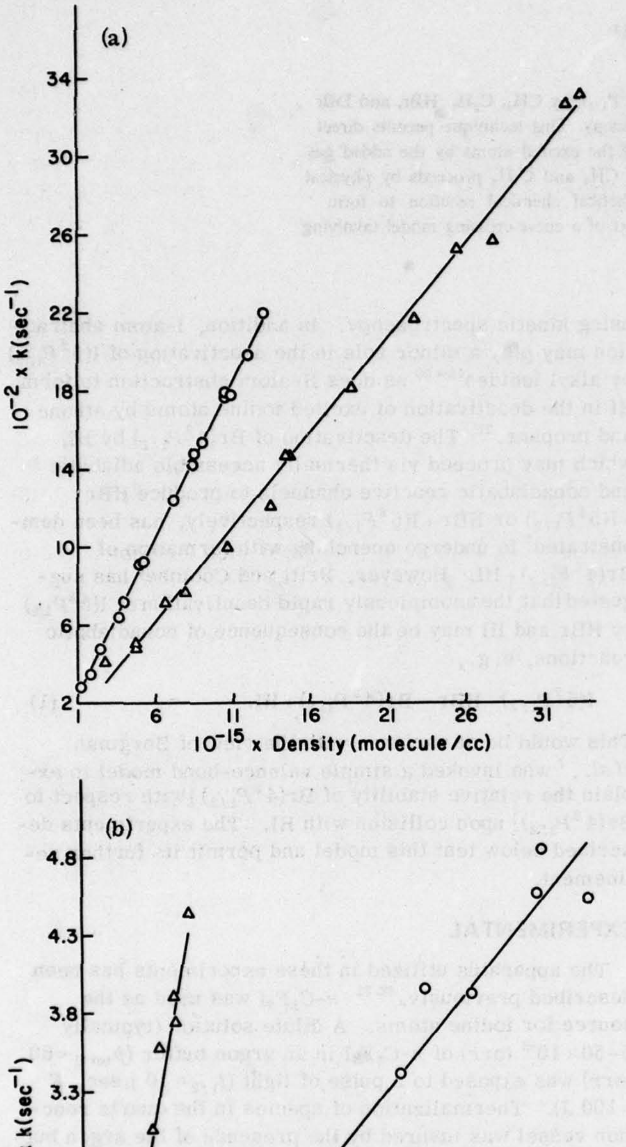

FIG. 1. Plots of pseudo-first order rate constants for removal of I(5 $^2P_{1/2}$) vs density of deactivating gas. (a) ○ C_3H_8, △ CH_4; (b) ○ DBr, △ HBr.

Samples of n-C_3F_7I (PCR, Inc.) were first degased and then purified by repeated distillations from a chlorobenzene slush (228 °K) to liquid N_2. Research grade H_2 (Matheson) was used without further purification. Ultra-high purity argon (Matheson) was passed over a molecular sieve at 193 °K immediately before use. HBr (99.8%, Matheson) was degassed and repeatedly distilled from ethanol slush (159 °K) to liquid N_2. DBr (99 at. % deuterium, Merck Sharp & Dohme Isotopes) was similarly purified. DBr was also stored at 240 °K prior to use. Research grade C_3H_8 (Matheson) was purified by several distillations from ethanol slush to liquid N_2. Research grade CH_4 (Phillips 66) was thoroughly degassed before use.

All mixtures were prepared on a Hg-free glass vacuum line which was evacuable to ~10^{-6} torr. The composition of the gas mixture in the reaction vessel was determined by use of calibrated floating ball rotameters. Pressures were measured with a glass Bourdon gauge and standard test gauges. This vacuum system was exposed to DBr before preparation of mixtures including this gas in order to passivate the exposed surfaces to H-atom exchange.

RESULTS

The initial experimental study described here involved the determination of the overall rate constant at 295 °K for the collisional deactivation of I* by the gases H_2, CH_4, C_3H_8, HBr, and DBr. The removal of I* was monitored using the resonance transition at 206.3 nm, the absorption signal being related to $[I^*]_t$ by

$$\ln I_0/I_t = \epsilon(l[I^*]_t)^\gamma, \qquad (2)$$

where the constants have previously been described.[25] The intensity of the radiation passing through the vessel, I_0, before the flash was obtained using the pretrigger record feature of the Transient Recorder. An experimental value of γ (typically 0.72–0.88) was determined over the range of observed absorption using the technique discussed below. The pseudo-first-order rate coefficient k derived from the transient absorption measurements ($[Q] \gg [I^*]_t$) may be related to the bimolecular rate constant k_Q by

$$k = k_Q[Q] + K,$$

where K represents removal of I* by spontaneous emission, diffusion to the walls of the reaction vessel, and quenching by impurities in the samples of n-C_3F_7I and argon buffer.

The results of these experiments are presented in Fig. 1 and Table I. Inspection of Table I suggests that the current results are in very good agreement with those obtained in other laboratories thus confirming the utility of the modified Beer–Lambert Law (2) in relating the observed transmission of resonance radiation through the reaction vessel to the concentration of transient species present.

TABLE I. Rate coefficients for deactivation of $I(5\,^2P_{1/2})$ at 295 °K.

Q	K_Q (cm^3 molecule^{-1} sec^{-1})	Ref.
CH_4	$1.0 \pm 0.2 \times 10^{-13}$	a
	$1.1 \pm 0.5 \times 10^{-13}$	b
	$9.7 \pm 0.3 \times 10^{-14}$	This work
C_3H_8	$1.7 \pm 0.1 \times 10^{-13}$	a
	$1.9 \pm 0.3 \times 10^{-13}$	b
	$1.6 \pm 0.1 \times 10^{-13}$	This work
HBr	$1.3 \pm 0.1 \times 10^{-13}$	c
	$1.6 \pm 0.1 \times 10^{-13}$	d
	$1.5 \pm 0.1 \times 10^{-13}$	This work
DBr	$\leq 4.9 \pm 0.3 \times 10^{-14}$	c
	$3.1 \pm 0.2 \times 10^{-14}$	This work

[a] D. Husain and J. R. Wiesenfeld, Trans. Faraday Soc. 63, 1349 (1967).

[b] J. J. Deakin and D. Husain, J. Chem. Soc. Faraday 2, 68, 41 (1972).

[c] Reference 6.

[d] Reference 8.

Determination of the overall rate constant described above does not yield information concerning the mechanism by which deactivation occurs. Rather, it is necessary to monitor the products of either Reaction (1), the chemical removal of I* by HBr, and/or the quenching process

$$I(5\,^2P_{1/2}) + HBr \rightarrow I(5\,^2P_{3/2}) + HBr^{(\dagger)}, \tag{3}$$

the yield of reaction then being expressed as $\Lambda = k_1/(k_1 + k_3)$. The measurement of Λ was carried out by monitoring the concentration of ground state I at 178.3 nm during the course of the following experiments:

(a) A given pressure of n-C_3F_7I was photolyzed in the absence of all gases other than the argon buffer [Fig. 2(a)]. The absorption measured immediately following the photolytic flash thus represented $[I]_{t=0}$, the amount of ground state iodine atoms produced photolytically.

(b) Addition of an excess of H_2 to the photolysis mixture described in (a) resulted in the relatively rapid $\{\tau = (k_{H_2}[H_2])^{-1} \sim 10^{-3}-10^{-4}\ \text{sec})\}$ relaxation of I* produced in the flash to form I. It should be noted that collisional deactivation of I* by H_2 must proceed via quenching to ground state atoms as reaction to form H + HI is 11.2 kcal endothermic. Hence, the absorption immediately following the flash [Fig. 2(b)] may be related to the total production of iodine atoms, $[I^*]_{t=0} + [I]_{t=0}$.

(c) Replacement of the H_2 by HBr (or other deactiviating molecule under investigation) so that $k_{H_2}[H_2] \approx k_{HBr}[HBr]$ permits direct measurement of the ground state iodine atoms produced by quenching of I* by the HBr in Process (3). If the absorption at 178.3 nm is significantly smaller than that obtained following quenching by H_2, it may be inferred that a significant fraction of the deactivation proceeds via chemical Reaction (1). This is demonstrated in Fig. 2(c).

While the results displyed in Fig. 2 clearly show that $k_1 > k_3$, quantitative information must be obtained from a detailed analysis of the kinetic scheme characterizing the transient species present in the reaction vessel. Such a scheme may be represented by

$$I^* + HX \rightarrow I + HX, \tag{3}$$

$$I^* + HX \rightarrow HI + X, \tag{1}$$

$$I^* \rightarrow I, \tag{4}$$

$$I \xrightarrow{\text{wall}} \tfrac{1}{2}I_2, \tag{5}$$

where $k_4 = \beta'/P_{Ar} + A_{nm} + k_Q[Q]$, Q being a trace impurity in the argon buffer. The term β'/P_{Ar} represents deactivation to I following diffusion to the vessel walls. Under the experimental conditions used, Processes (1) and (3) would display pseudo-first-order kinetics so $k'_1 = k_1[HX]$ and $k'_3 = k_3[HX]$. The kinetic equations

$$d[I^*]/dt = -(k'_1 + k'_3 + k_4)[I^*],$$

$$d[I]/dt = (k'_3 + k'_4)[I^*] - k_5[I]$$

may be integrated yielding

$$[I^*]_t = [I^*]_{t=0} \exp[-(k'_1 + k'_3 + k_4)t], \tag{6}$$

$$[I]_t = \frac{(k'_3 + k_4)[I^*]_{t=0}}{k_5 - k'_1 - k'_3 - k_4}\left[e^{-(k'_1 + k'_3 + k_4)t} - e^{-k_5 t}\right] + [I]_{t=0}\, e^{-k_5 t}. \tag{7}$$

Since $k'_1 + k'_3 + k_4 \gg k_5 \sim \beta'/P_{Ar}$, at times long compared to $(k'_1 + k'_3 + k_4)^{-1}$ Eq. (7) reduces to

$$[I]_t \approx e^{-k_5 t}\left\{\frac{-(k'_3 + k_4)[I^*]_{t=0}}{k_5 - k'_1 - k'_3 - k_4} + [I]_{t=0}\right\}.$$

Thus, a plot of $\ln[I]_t$ vs time should be linear with slope $-k_5$ and intercept α

$$\alpha = \frac{-(k'_3 + k_4)[I^*]_{t=0}}{k_5 - k'_1 - k'_3 - k_4} + [I]_{t=0}\,.$$

Such a relationship is indeed observed for the temporal profiles of ground state iodine atom concentrations for the experiments done in the presence of H_2 or other deactivating molecules discussed here. Substitution for k_4 and rearrangement yields

$$\frac{\alpha - [I]_{t=0}}{[I^*]_{t=0}} = \frac{-(k'_3 + k_4)}{k_5 - (k'_1 + k'_3 + \beta'/P_{Ar} + k_Q[Q] + A_{nm})}\,. \tag{8}$$

As noted above $k_5 \sim \beta'/P_{Ar}$. Furthermore, $k'_1 + k'_3 \gg k_Q[Q] + A_{nm}$. Finally, the numerator of (8) may be simplified by the assumption $k'_3 \gg k_4$ which is valid so long as k'_3 is not much smaller than k'_1, i.e., some appreciable fraction of the deactivating collisions result in quenching rather than reaction. If reaction is, on the other hand, overwhelmingly predominant the following analysis yields only a lower limit on the true value of Λ.

Equation (8) now becomes

$$\frac{\alpha - [I]_{t=0}}{[I^*]_{t=0}} = \frac{k'_3}{k'_1 + k'_3} = 1 - \Lambda. \tag{9}$$

Referring to the earlier description of the experimental sequence and recalling the modified Beer–Lambert Law, we define $A_0 = \ln(I_0/I)_{t=0} = \epsilon(l[I]_{t=0})^{\gamma}$ as the absorbance immediately following the photolysis of n-C_3F_7I in the absence of an added quencher, $A_{H_2} = \epsilon[l([I]_{t=0} + [I^*]_{t=0})]^{\gamma}$ as the absorbance measured in the presence of H_2 and $A_{HX} = \epsilon(l\alpha)^{\gamma}$ as the absorbance determined in the presence of a potential reactant. Substitution into (9) now yields

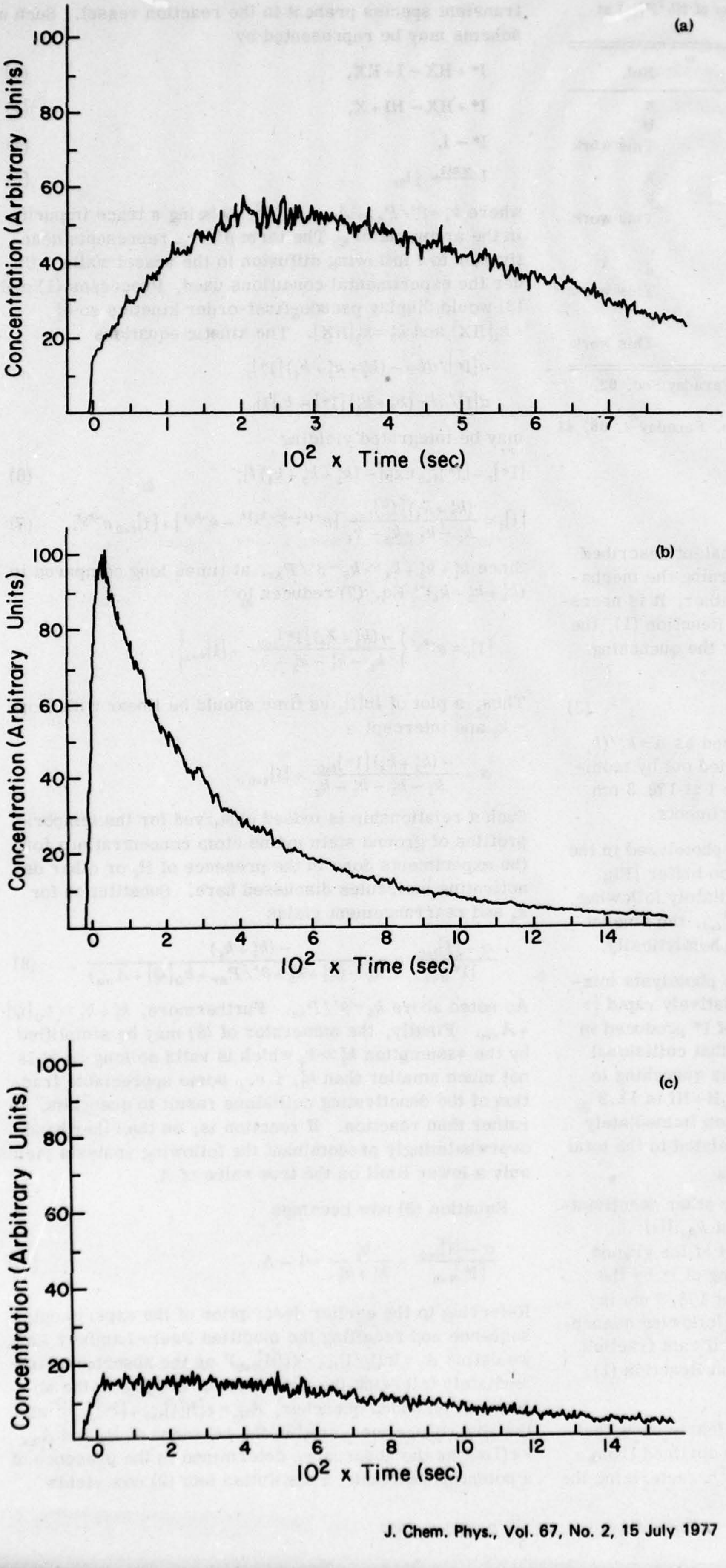

FIG. 2. Temporal profiles of $I(5\,^2P_{3/2})$ following photolysis of a solution of n-C_3F_7I in argon ($P_{n\text{-}C_3F_7I} = 0.019$ torr, $P_{Ar} = 60$ torr, $E = 100$ J). The different solutions included: (a) no added deactivating gas; (b) 0.37 torr H_2 to quench all $I(5\,^2P_{1/2})$ rapidly to $I(5\,^2P_{3/2})$; (c) 0.25 torr HBr, a deactivator of unknown reactivity in the presence of $I(5\,^2P_{1/2})$. These traces, each representing the average of 16 kinetic runs, demonstrate the dominance of Reaction (1) in the deactivation of $I(5\,^2P_{1/2})$ by HBr.

TABLE II. Fraction of deactivating collisions resulting in chemical reaction.

Q	Λ(Eq. 10)
CH_4	0.03 ± 0.11
C_3H_8	0.03 ± 0.16
HBr	0.96 ± 0.12
DBr	0.94 ± 0.13

$$\Lambda = 1 - (A_{HX}^{\gamma^{-1}} - A_0^{\gamma^{-1}})/(A_{H_2}^{\gamma^{-1}} - A_0^{\gamma^{-1}}). \quad (10)$$

The averaged values of Λ summarized in Table II were obtained by evaluating the experimental absorbances at 178.3 nm following photolysis of n-C_3F_7I in the absence of any added quencher, with H_2 and with HX. A given set of three runs were included in the overall average if the partial pressure of n-C_3F_7I was maintained to $\pm 1\times10^{-3}$ torr. As noted previusly,[25] in the limit where the n-C_3F_7I may be regarded as an optically thin absorber and the concentration of ground and excited state iodine atoms produced in the flash is proportional to the partial pressure of n-C_3F_7I,

$$[I^{(*)}]_{t=0} = \kappa^{(*)} P_{n\text{-}C_3F_7I} \quad (11)$$

(κ reflects the photolytic yield of iodine atoms), substitution of (11) into (2) yields

$$\ln\ln(I_0/I)_{t=0} = \text{const} + \gamma \ln P_{n\text{-}C_3F_7I}. \quad (12)$$

Plots of $\ln A_x$ where $A_x = A_0$, A_{H_2} or A_{HX} vs $\ln P_{n\text{-}C_3F_7I}$ derived from the present experimental data (Figs. 3–6) verify this relationship over the range of absorbances measured as well as yielding required values for γ used in the evaluation of (10). It may further be shown that

$$\Lambda = 1 - \frac{\exp(\Omega_{HX}/\gamma) - \exp(\Omega_0/\gamma)}{\exp(\Omega_{H_2}/\gamma) - \exp(\Omega_0/\gamma)}, \quad (13)$$

where Ω_x is the constant in (12). Evaluation of (13) leads to values of Λ in good agreement with those obtained by use of (10), but errors introduced by slow long-term drifts in flash lamp output and resonance lamp profile which are avoided by calculating Λ using data points collected over a short period of time leads to a larger scatter in the final results.

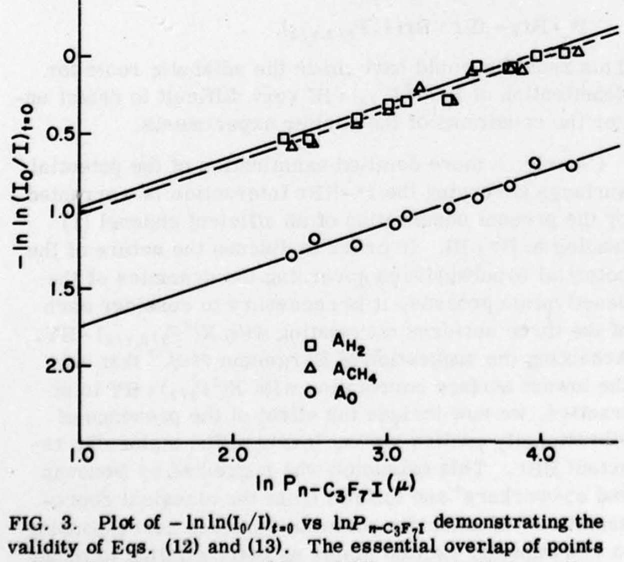

FIG. 3. Plot of $-\ln\ln(I_0/I)_{t=0}$ vs $\ln P_{n\text{-}C_3F_7I}$ demonstrating the validity of Eqs. (12) and (13). The essential overlap of points collected in the presence of H_2 and CH_4 suggests that reaction plays no role in the deactivation of I($5\,^2P_{1/2}$) by CH_4. For the sake of clarity, only a random selection of the actual data taken is presented here.

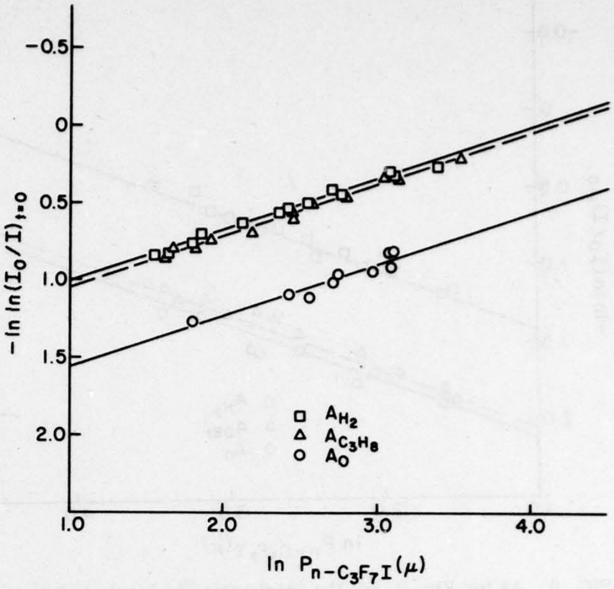

FIG. 4. As for Fig. 3, but the deactivating molecule is C_3H_8. No significant degree of reactive deactivation is observed.

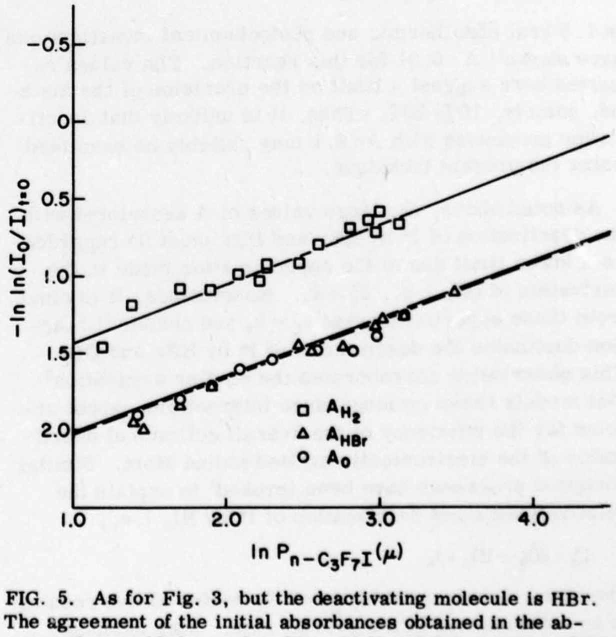

FIG. 5. As for Fig. 3, but the deactivating molecule is HBr. The agreement of the initial absorbances obtained in the absence of any added quencher [Fig. 2(a)] and the presence of HBr [Fig. 2(c)] is the result of chemical reaction between I($5\,^2P_{1/2}$) and the deactivating gas.

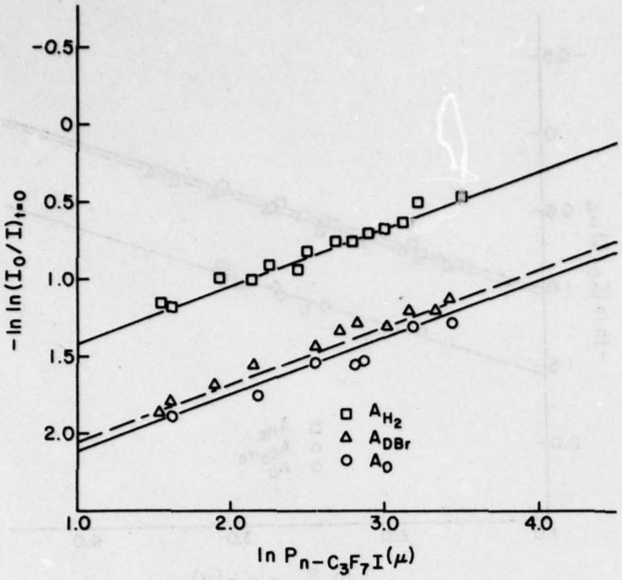

FIG. 6. As for Fig. 3, but the deactivating molecule is DBr. Once again, chemical reaction is the major channel for collisional deactivation.

DISCUSSION

The examination of CH_4 and C_3H_8 as deactivating gases was carried out in order to assess the precision of the experimental technique outlined above. Neither of these gases is expected to react appreciably with I*, hydrogen abstraction from CH_4,

$$I^* + CH_4 \rightarrow HI + CH_3$$

being 11.0 kcal endothermic. Abstraction of a secondary hydrogen from C_3H_8

$$I^* + C_3H_8 \rightarrow i\text{-}C_3H_7\cdot + HI$$

is 1.5 kcal endothermic and photochemical investigations have shown[21] $\Lambda < 0.01$ for this reaction. The values reported here suggest a limit on the precision of the method, namely, 10%–20%. Thus, it is unlikely that deactivation processes with $\Lambda < 0.1$ may reliably be examined using the present technique.

As noted above, the large values of Λ associated with the deactivation of I* by HBr and DBr must be regarded as a lower limit due to the approximation made in the derivation of (9), i.e., $k_3' \gg k_4$. Nonetheless, it is clear from these experiments that $k_1 \gg k_3$ and chemical reaction dominates the deactivation of I* by HBr and DBr. This observation corroborates the earlier suggestion[8] that models based on long-range interactions cannot account for the efficiency of the overall collisional deactivation of the electronically excited iodine atom. Similar chemical processes have been invoked[1] to explain the relatively efficient deactivation of I* by HI, i.e.,

$$I_a^* + HI_b \rightarrow HI_a + I_b,$$

where the chemical exchange of the iodine atoms results in an enhancement of the overall rate. Such exchange reactions have been suggested in the case of the efficient vibrational deactivation of vibrationally excited hydrogen halides by halogen atoms.[26] Indeed, the present experimental results may be used to assess the effect of electronic excitation on the rate of chemical reaction. Thus, if the activation energy for the reaction of ground state iodine atoms with HBr

$$I + HBr \rightarrow HI + Br \quad \Delta H = +16.2 \text{ kcal},$$

is assumed to be equal to the endothermicity, it is possible to estimate the fraction of electronic excitation energy made available to the collision partners to surmount the activation barrier. If the cross section for a gas kinetic I–HBr collision is ~16 Å^2 (based on Xe–Kr collision diameters)[27] and the nominal steric factor is taken as unity, the observed rate constant for (1), 1.5×10^{-13}, may be interpreted as being associated with a maximum activation energy of 4.3 kcal. Thus, 11.9 kcal or 55% of the 21.7 kcal excitation energy associated with $I(5\,^2P_{1/2})$ is made available to the collision complex. This reflects a lower limit, however, for the actual preexponential factor is <1.

The absence of a *large* energy barrier to reaction may now be viewed in the context of simple models based on the electronic structure of the IHBr collision complex. Turning first to the one-electron valence bond approach developed[7] to explain the efficient quenching of $Br(4\,^2P_{1/2})$ by HI where neither adiabatic nor nonadiabatic chemical reaction appears to play a significant role, it seems clear that a serious discrepancy is raised by the current results. Inspection of Fig. 4 of Ref. 7, would suggest that the initial approach of I* to HBr should take place on a strongly repulsive surface. Therefore, any reactive process which requires a close approach of the reactants should display a significant activation barrier and, in addition, would be expected to be relatively inefficient with respect to long-range processes such as energy transfer. The applicability of this simple model has been further challenged by recent experimental work[28] which demonstrated that the original studies[7] failed to account for the rapid reaction

$$I^* + Br_2 \rightarrow IBr + Br(4\,^2P_{1/2,3/2}).$$

This reaction would have made the adiabatic route for deactivation of $Br(4\,^2P_{1/2}) + HI$ very difficult to detect under the conditions of the earlier experiments.

Clearly, a more detailed examination of the potential surfaces governing the I*–HBr interaction is warranted by the present observation of an efficient channel (1) leading to Br + HI. In order to discuss the nature of the potential hypersurfaces governing the dynamics of the deactivation process, it is necessary to consider each of the three surfaces correlating with $X(^2P_{3/2,1/2}) + HY$. Accepting the suggestion of Bergmann *et al.*[7] that only the lowest surface correlating with $X(^2P_{3/2}) + HY$ is attractive, we now include the effect of the presence of vibrationally excited virtual levels of the molecular reactant HBr. This extension was suggested by Donovan and co-workers[6] and follows from the classical representation[29] of adiabatic potential surfaces corresponding to vibrationally excited states as being similar to those correlating with the ground state, but being displaced upward in energy by $h\nu_{vib}$. The nature of the potential hypersurfaces near the nuclear arrangement corresponding

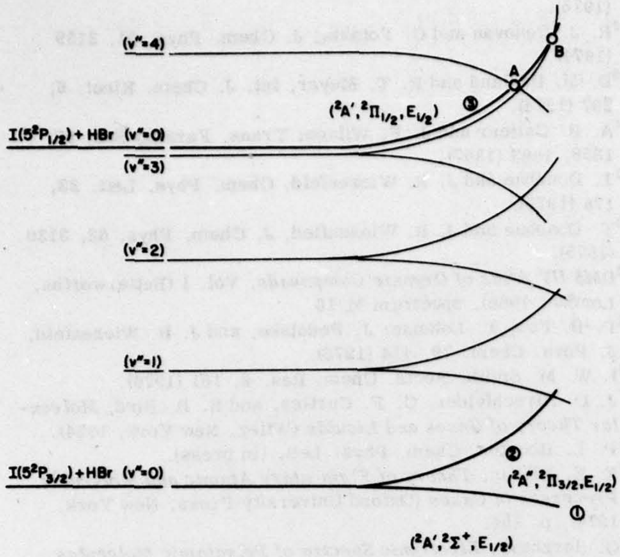

FIG 7. Schematic drawing of the potential surfaces governing the interaction between iodine atoms and HBr. Type 1 surfaces correlate to Br(4 $^2P_{3/2}$) + HI via a surface which is essentially bonding. Type 2 surfaces correlate with the same products but are presumably nonbonding at large internuclear distances and somewhat repulsive at close approach. The type 3 surface correlates with Br(4 $^2P_{1/2}$) + HI and is also nonbonding in nature. At point A, it undergoes an avoided crossing (for the case of j, Ω coupling) with the virtual surface correlating with vibrationally excited HBr; this type 1 surface leads to chemical reaction. The avoided crossing at B, which is suggested here to occur at higher energies, leads to formation of I(5 $^2P_{3/2}$) and is presumably of no significance in the present reaction.

to reactant I + HBr is presented schematically in Fig. 7. Here, the symmetry of the curves are given for the cases of weak spin–orbit coupling and symmetries of the intermediate complex which are either planar ($^2A'$ or $^2A''$) or axial ($^2\Sigma^+$, $^2\pi_{1/2,3/2}$) as well as strong spin–orbit coupling (all surfaces of $E_{1/2}$ representation[30]). Surfaces designated as *type 1 lead to Br + HI and are characterized by an attractive interaction.* Surfaces 2 and 3 are nonbonding at large internuclear separations and possibly repulsive at close approach.

The regions of greatest concern to the present discussion center around the crossings of the hypersurface correlating with the reactants I* + HBr (type 3) and those correlating with I + HBr ($v''=3$) (type 2) and I + HBr ($v''=4$) (type 1). These crossings are avoided for the case of j, Ω coupling where all surfaces are represented by $E_{1/2}$ in the extended $C_{\infty v}$ point group. As chemical reaction and not physical quenching has been shown to be the dominant route for collisional deactivation of I* by HBr, clearly the region near the crossing (point A) between the surface correlating with I* + HBr ($v''=0$) and that correlating with I + HBr ($v''=4$) must be of primary importance. The failure to observe a significant channel to ground state iodine atoms suggests that the crossing between the surface emanating from I* + HBr ($v''=0$) with the surface correlating with I + HBr ($v''=3$) (point B) must occur at an energy not available to a significant fraction of the colliding reactants at 295 °K. As the crossing at A is avoided, it is perhaps surprising that the overall rate constant for reaction, $1.5 \pm 0.1 \times 10^{-13}$ cm^3 molecule^{-1} sec^{-1}, is not larger. Of course, a small activation barrier to reaction may indeed be present, 4 kcal being the maximum possible. However, it must also be recalled that the probability for nonadiabatic passage through the avoided crossing at point A must be relatively large. This is due to the need to include the vibrational overlap between the initial and final states in the calculation of the overall matrix element $V(R_A)$ for transition from the $v''=0$ level of the type 3 surface to the $v''=4$ level of the type 1 surface,

$$V_{0,4}(R_A) = V_{el}(R_A)\,[q_{0,4}(R_A)]^{1/2},$$

where V_{el} *is the electronic part of the matrix element at* R_A and q represents the Frank–Condon factor for the vibrational overlap.[31] The rate constants for deactivation of I* by HBr and DBr, $k_{HBr}/k_{DBr} = 4.7$, is not inconsistent with this interpretation as the matrix element would involve $q_{0,5}$ which would be significantly smaller than the Frank–Condon factor for the 0–4 transition. The magnitude of the potential barrier to the region of avoided crossing at A and B will be assessed in temperature-controlled experiments to be undertaken in this laboratory.

It is interesting to note that the proposed model discussed above suggests that the products of (1) are formed in a concerted reaction following initial production of HBr ($v''=4$) + I. The observed reaction cannot be the result of the following two-step mechanism

$$\mathrm{I^* + HBr}(v''=0) \rightarrow \mathrm{I + HBr}(v''=4),$$

$$\mathrm{I + HBr}(v''=4) \rightarrow \mathrm{HI + Br}$$

as the second step would be in competition with the rapid vibrational process

$$\mathrm{HBr}(v''=4) + \mathrm{HBr}(v''=0) \rightarrow \mathrm{HBr}(v''=3) + \mathrm{HBr}(v''=1), \text{ etc.}$$

and [HBr] ~ 10^4–$10^5 \times$[I]. The nascent energy distribution of the HI($v''=n$) + Br should correspond to that which would have been obtained following the reaction of vibrationally excited HBr with ground state iodine atoms. Observation of the vibrational energy disposition in the products of this reaction would greatly facilitate the evaluation of the proposed mechanism. Furthermore, such an experiment would permit the assessment of the role of reactant vibrational energy in chemical processes. It should be noted that failure to observe the ground state iodine atom suggests that there is no remaining thermal barrier to reaction to form Br + HI once the path of avoided crossing is taken at point A.

ACKNOWLEDGMENT

This work was supported by the Office of Naval Research.

---

[1] D. Husain and R. J. Donovan, Adv. Photochem. 8, 1 (1971).

[2] R. J. Donovan and H. M. Gillespie, *Specialist Periodical Report, Reaction Kinetics*, Vol. I (Chemical Society, London, 1975), p. 14.

[3] F. J. Wodarczyk and P. B. Sackett, Chem. Phys. 12, 65 (1976).

[4] S. R. Leone and F. J. Wodarczyk, J. Chem. Phys. 60, 314 (1974).

[5] R. J. Butcher, R. J. Donovan, and R. H. Strain, J. Chem. Soc. Faraday Trans. 2, 70, 1837 (1974).

[6] R. J. Donovan, C. Fotakis, and M. F. Golde, J. Chem. Soc. Faraday Trans. 2, 72, 2055 (1976).

[7] K. Bergmann, S. R. Leone, and C. B. Moore, J. Chem. Phys 63, 4161 (1975).

[8] A. T. Pritt, Jr., and R. D. Coombe, J. Chem. Phys. 65, 2096 (1976).

[9] J. R. Wiesenfeld and G. L. Wolk, J. Chem. Phys. 65, 1506 (1976).

[10] A. B. Peterson, C. Witting, and S. R. Leone, Appl. Phys. Lett. 27, 305 (1975).

[11] J. J. Ewing, Chem. Phys. Lett. 29, 50 (1974).

[12] R. D. Sharma and C. A. Brau, Phys. Rev. Lett. 19, 1273 (1967).

[13] R. V. Sharma and C. A. Brau, J. Chem. Phys. 50, 924 (1969).

[14] I. H. Zimmerman and T. F. George, Chem. Phys. 7, 323 (1975).

[15] I. H. Zimmerman and T. F. George, J. Chem. Soc. Faraday Trans. 2 71, 2030 (1975).

[16] R. J. Donovan, F. G. M. Hathorn, and D. Husain, Trans. Faraday Soc. 64, 3192 (1968).

[17] F. G. M. Hathorn and D. Husain, Trans. Faraday Soc. 65, 2678 (1969).

[18] T. Donohue and J. R. Wiesenfeld, J. Phys. Chem. 80, 437 (1976).

[19] R. J. Donovan and C. Fotakis, J. Chem. Phys. 61, 2159 (1974).

[20] D. M. Haaland and R. T. Meyer, Int. J. Chem. Kinet. 6, 297 (1974).

[21] A. B. Callear and J. F. Wilson, Trans. Faraday Soc. 63, 1358, 1983 (1967).

[22] T. Donohue and J. R. Wiesenfeld, Chem. Phys. Lett. 33, 176 (1975).

[23] T. Donohue and J. R. Wiesenfled, J. Chem. Phys. 63, 3130 (1975).

[24] *DMS UV Atlas of Organic Compounds*, Vol. I (Butterworths, London, 1966), spectrum M/10.

[25] P. D. Foo, T. Lohman, J. Podolske, and J. R. Wiesenfeld, J. Phys. Chem. 79, 414 (1975).

[26] I. W. M. Smith, Accts. Chem. Res. 9, 161 (1976).

[27] J. O. Hirschfelder, C. F. Curtiss, and R. B. Bird, *Molecular Theory of Gases and Liquids* (Wiley, New York, 1954).

[28] P. L. Houston, Chem. Phys. Lett. (in press).

[29] E. E. Nikitin, *Theory of Elementary Atomic and Molecular Processes in Gases* (Oxford University Press, New York, 1974), p. 154.

[30] G. Herzberg, *Electronic Spectra of Polyatomic Molecules* (Van Nostrand, Princeton, 1967), p. 14.

[31] E. Bauer, E. R. Fisher, and F. R. Gilmore, J. Chem. Phys. 51, 4173 (1969).

Volume 50, number 3 CHEMICAL PHYSICS LETTERS 15 September 1977

LASER INDUCED PHOTODISSOCIATION SPECTROSCOPY: Br_2

T.G. LINDEMAN and J.R. WIESENFELD ‡
Department of Chemistry, Cornell University,
Ithaca, New York 14853, USA

Received 26 May 1977

The continuous absorption spectrum of molecular bromine has been examined using laser induced photodissociation spectroscopy. In this technique, Br_2 molecules are photolyzed using a flashlamp-pumped dye laser; the atomic products of the dissociation are then monitored by time-resolved resonance absorption spectroscopy in the vacuum ultraviolet. The relative absorptivities for the transitions $B\,^3\Pi_{0^+u} \leftarrow X\,^1\Sigma_g^+$ and $^1\Pi_{1u} \leftarrow X\,^1\Sigma_g^+$ have been obtained at 18350, 21010 and 22125 cm^{-1}.

1. Introduction

The spectra and electronic structure of halogen molecules have been extensively investigated [1]. The information obtained about the low-lying excited states of these molecules has led to the development of our understanding of the spectroscopic basis of photochemistry. While most experimental observations have been carried out on I_2, the other halogens have also been investigated. In particular, the spectrum of Br_2 has been studied [2], both in the banded region below the thermochemical threshold for formation of $Br(4\,^2P_{1/2})$ + $Br(4\,^2P_{3/2})$, 19580 cm^{-1}, and more recently in the continuum region where the significant transitions are $B\,^3\Pi_{0^+u} \leftarrow X\,^1\Sigma_g^+$ and $^1\Pi_{1u} \leftarrow X\,^1\Sigma_g^+$, the $^3\Pi_{0^+u}$ state correlating with $Br(4\,^2P_{1/2})$ + $Br(4\,^2P_{3/2})$ and the $^1\Pi_{1u}$ with two $Br(4\,^2P_{3/2})$.

The experiments on Br_2 spectroscopy have not, in general, been accompanied by corresponding quantitative investigations of halogen photochemistry. In particular, the actual yields of $Br(4\,^2P_{1/2})$ and $Br(4\,^2P_{3/2})$ following the photolysis of Br_2 have only recently been reported for a set of discrete photolytic wavelengths [3]. These experiments were carried out using the elegant technique of photofragment spectroscopy, where both the translational energy and the angular distribution of photolysis products with respect to the polarization angle of the incoming actinic radiation are obtained. Analysis of these data yields both the relative efficiencies for the production of specific quantum states of the atom as well as the symmetry of the spectroscopic transition leading to photodissociation. Measurements of the relative yields of electronically excited and ground state Br atoms have been made at relatively few wavelengths, and substantial disagreement exists between results obtained by direct observation of products [3] and those derived from analysis of the temperature dependence of the Br_2 absorption spectrum [2]. The experiments described here were carried out in order to resolve this discrepancy and to test the validity of the spectral analysis method.

2. Experimental

Fig. 1 is a schematic diagram of the apparatus used for laser induced photodissociation spectroscopy. The photolysis of the source molecule was accomplished in a Pyrex vessel of 20 cm length with an internal square cross section of 1.0 cm. The output of the laser beam was directed through the vessel, whose polished walls were externally coated with an Al film. Approximately 20–25 reflections were made as the light was transmitted through the length of the square cell, resulting in a

---

‡ Henry and Camille Dreyfus Teacher–Scholar.

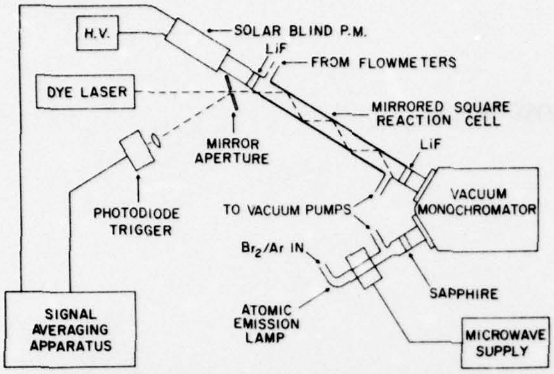

Fig. 1. Schematic diagram of experimental apparatus.

total pathlength of ca. 28 cm. The Br_2 source gas was prepared in a very dilute solution with ultra high purity argon (Matheson) which was passed over molecular sieve at 195 K immediately prior to use. The argon served both as a thermal buffer and to slow the rate of atomic diffusion to the walls of the vessel. The gases in the reaction cell were swept out in a time short compared to the period between laser pulses (3–8 s) but long compared to the characteristic time for diffusion (ca. 20 ms).

The dye laser (model 1200, phase-R) was pumped by a fast coaxial flashlamp and produced output pulses of 100–200 ns duration. A number of dyes (table 1) were utilized in these experiments in order to permit observation of photodissociation products following exposure to a range of actinic wavelengths. The laser cavity consisted of two broad band mirrors; in these initial experiments no effort was made to tune the laser over narrow spectral regions. Output energies of 10–30 mJ were achieved with dyes listed; the relatively modest power levels attained, i.e., ≈100 kW suggest that two-photon processes should not play a significant role in these experiments.

The temporal profiles of ground state, $Br(4\,^2P_{3/2}) \equiv Br$, and electronically excited, $Br(4\,^2P_{1/2}) \equiv Br^*$, bromine atom concentrations were monitored using time-resolved atomic absorption spectroscopy. The atomic resonance radiation was produced in a microwave-powered electrodeless discharge lamp through which flowed ca. 0.3 torr of a 1% Br_2/Ar mixture. Incident power was 18 W. The output of the resonance lamp (fig. 2) was then dispersed using a 0.3 M vacuum monochromator (McPherson 218) and detected by an EMI G26E3-15 solar blind photomultiplier. The ground and excited states of bromine were detected by attenuation of the resonance transitions, $5\,^2P_{3/2} \leftarrow 4\,^2P_{3/2}$ (148.9 nm) and $5\,^2P_{1/2} \leftarrow 4\,^2P_{1/2}$ (153.2 nm), respectively. Transient absorption signals following the laser pulse were digitized using a Biomation 802 transient recorder and then averaged to enhance the observed signal-to-noise ratio. Typically 16–64 kinetic runs were averaged.

Table 1
Relative absorptivities for $B\,^3\Pi_{0^+u} \leftarrow X\,^1\Sigma_g^+$ and $^1\Pi_{1u} \leftarrow X\,^1\Sigma_g^+$ transitions in Br_2

Laser dye	$\nu(cm^{-1})$	$\epsilon(^3\Pi)/\epsilon(^1\Pi)$
P495	18350 ± 250	0.4
coumarin 102	21010 ± 275	13
coumarin 2	22125 ± 100	1.8

Ultrapure Br_2 (99.9%, Ventron) was extensively degassed. Research grade H_2(Matheson) was used as received. All mixtures were prepared on a mercury-free vacuum system, evacuable to 10^{-6} torr and equipped with a capacitance manometer and stainless steel test gauges. The partial pressures of reagents in the photolysis cell were determined from the total pressure (20–35 torr) and relative flow rates measured with calibrated rotameters. The pressure of Br_2 varied in the range 0.008–0.030 torr; that of H_2 was either 0 or between 0.040 and 0.10 torr.

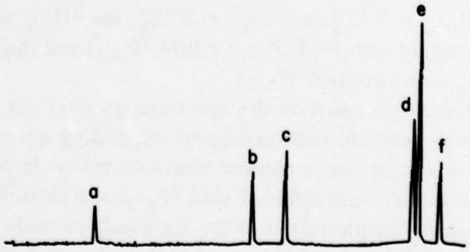

Fig. 2. Output spectrum of bromine resonance lamp. Transitions are (a) $4\,^2P_{3/2} \leftarrow 5\,^2P_{3/2}$, 148.9 nm, (b) $4\,^2P_{1/2} \leftarrow 5\,^2P_{1/2}$, 153.2 nm, (c) $4\,^2P_{1/2} \leftarrow 5\,^4P_{3/2}$, 154.1 nm, (d) $4\,^2P_{1/2} \leftarrow 5\,^2P_{3/2}$, 157.5 nm, (e) $4\,^2P_{3/2} \leftarrow 5\,^4P_{5/2}$, 157.7 nm, and (f) $4\,^2P_{1/2} \leftarrow 5\,^4P_{1/2}$, 158.2 nm. Transitions (a) and (b) were used in these experiments.

3. Results and discussion

In order to test the experimental arrangement described above, the overall rate of Br* deactivation upon collision with Br_2 was determined. This was accomplished by monitoring the 153.2 nm resonance line following laser photolysis of Br_2. The absorption of resonance radiation may be related to the concentration of Br* atoms through the use of the Beer–Lambert law

$$\ln(I_0/I)_t = \epsilon(l\,[X])^{\gamma},$$

where X = Br*. The value of the exponent, γ, which relates the observed transmission to the relative atomic concentration was determined experimentally [4] to be 1.0 in this apparatus. The measurement of k_{Br_2} was carried out by determining the pseudo-first order rate coefficients, k, for Br* deactivation in an excess of Br_2(p_{Br_2} = 0.008–0.020 torr). The rate coefficient for Br* removal is given by

$$k = k_{Br_2}[Br_2] + K,$$

where K represents impurity quenching and diffusion to and deactivation at the walls of the photolysis cell. The value of k_{Br_2} obtained in these experiments (fig. 3), $(1.1 \pm 0.1) \times 10^{-12}$ cm^3 molecule^{-1}s^{-1}, compares very favorably with the values in the range (1.0–1.2) $\times 10^{-12}$ reported in infrared emission [5] experiments. An earlier measurement [6] made using photographic kinetic spectroscopy yielded $k_{Br_2} = 2 \times 10^{-11}$ cm^3 molecule^{-1} s^{-1}, in poor agreement with more recent data.

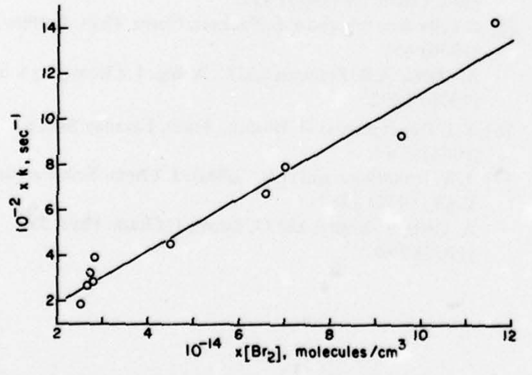

Fig. 3. Experimental results for rate of removal of Br* as a function of Br_2 density. Slope of the best-fit line yields k_{Br_2} (see text).

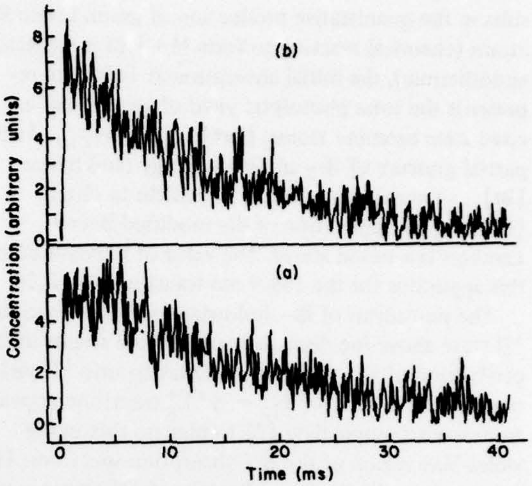

Fig. 4. Br-atom profiles following laser photolysis of Br_2 at 21010 cm^{-1}. p_{Br_2} = 0.012 torr, p_{Ar} = 19 torr. (a) p_{H_2} = 0, (b) p_{H_2} = 0.039 torr. Each trace represents average of 32 experimental runs.

The determination of relative adsorptivities for absorption via the $B\,^3\Pi_{0^+u} \leftarrow X\,^1\Sigma_g^+$ and $^1\Pi_{1u} \leftarrow X\,^1\Sigma_g^+$ transitions, $\epsilon(^3\Pi)/\epsilon(^1\Pi)$, was made by measuring the relative yields of Br and Br* following flash photolysis at a specific wavelength. The relative concentration of ground state bromine atoms was monitored at 148.9 nm under two experimental conditions. First, the temporal profile of bromine concentration, $[Br]_t$, was obtained in the absence of any added quencher of Br*. As may be seen from fig. 4a, this profile is characterized by a very rapid rise in Br concentration coincident with the laser pulse. This represents photolytic production of Br atoms from Br_2. The relatively level period then may be ascribed to physical quenching of Br* by Br_2 to form Br. This occurs on approximately the same time scale as diffusion of Br to the walls of this small photolysis vessel. This latter removal process dominates the Br-atom profile at long times, and results in heterogeneous recombination to form Br_2. Direct measurement of the absorption transient immediately following the laser pulse thus provides a relative photolytic yield of Br atoms.

The photolytic production of Br* is then determined by addition of 0.040–0.10 torr of H_2 to the photolysis vessel. This results in the deactivation of Br* on a time scale (ca. 15–20 μs) rapid with respect to that of the observation (fig. 4b). As deactivation of Br* by H_2 results in the quantitative production of ground state Br atoms (chemical reaction to form H + HBr is 6.2 kcal endothermic), the initial absorption at 148.9 nm represents the total photolytic yield of ground *and* excited state bromine atoms, $[Br^*]_{t=0} + [Br]_{t=0}$. As the partial pressure of Br_2 and laser energy (and hence $[Br]_{t=0}$) remain constant, it is possible to obtain $[Br^*]_{t=0}$ by application of the modified Beer–Lambert law noted above. The value of γ measured in this apparatus for the 148.9 nm transition was 0.76.

The photolysis of Br_2 following excitation into the $^3\Pi$ state above the dissociation threshold results in the production of Br* + Br while excitation into $^1\Pi$ yields two Br atoms. The $A\,^3\Pi_{1u} \leftarrow X\,^1\Sigma_g^+$ transition appears from spectroscopic data [2] to play no role in the violet-blue region of the Br_2 absorption spectrum. The relative absorptivities into the $^3\Pi$ and $^1\Pi$ continua may thus be related to the observed ground and excited-state Br atom yields,

$$\frac{\epsilon(^3\Pi)}{\epsilon(^1\Pi)} \propto \left[\frac{[Br]_{t=0}}{2[Br^*]_{t=0}} - 0.5\right]^{-1} .$$

The results obtained by application of this equation to experimental data taken at several photolysis wavelengths are presented in table 1. The values of $\epsilon(^3\Pi)/\epsilon(^1\Pi)$ are in sensible agreement with those derived from inspection of resolved spectral curves presented in previous reports [2,3]. Several points deserve more detailed discussion. The production of Br* following photolysis of Br_2 at 18350 ± 250 cm^{-1} cannot be due to direct photodissociation. Rather, its appearance may reasonably be ascribed to the effect of a collisional release process involving highly vibrationally excited $Br_2(B\,^3\Pi_{0^+u})$ which undergoes essentially thermal dissociation upon collision with Br_2 or Ar [7]. This phenomenon which has previously been demonstrated in I_2 [7], plays a significant role only in the region near the thermochemical threshold for production of Br + Br*; it need not be considered for photolysis above this energy.

The photolysis of Br_2 immediately above the dissociation threshold is dominated by excitation into the $B\,^3\Pi_{0^+u}$ state. This observation is in good agreement with previous spectral measurements [2] suggesting that the major component of the low energy maximum in Br_2 absorption near 20500 cm^{-1} is due to $B\,^3\Pi_{0^+u} \leftarrow X\,^1\Pi_g^+$. The dominance of this transition rapidly decreases at higher energies and, as may be seen from the results obtained at 22125 cm^{-1}, the $^1\Pi_{1u} \leftarrow X\,^1\Sigma_g^+$ transition will become the major component of the absorption below ca. 455 nm. The large change in the observed $\epsilon(^3\Pi)/\epsilon(^1\Pi)$ ratio over a short wavelength range, namely 475–452 nm suggests that similar experiments to those carried out here but involving a tunable laser cavity will yield significant information concerning the individual components of the absorption band. Such investigations are currently under way in this laboratory.

Acknowledgement

This work was generously supported by the U.S. Office of Naval Research.

References

[1] R.S. Mulliken, J. Chem. Phys. 55 (1971) 288.
[2] R.J. LeRoy, R.G. Macdonald and G. Burns, J. Chem. Phys. 65 (1976) 1485, and references therein.
[3] R.J. Oldman, R.K. Sander and K.R. Wilson, J. Chem. Phys. 63 (1975) 4252.
[4] P.D. Foo, T. Lohman, J. Podolske and J.R. Wiesenfeld, J. Phys. Chem. 79 (1975) 414.
[5] F.J. Wodarczyk and P.B. Sackett, Chem. Phys. Letters 12 (1976) 65;
A. Harri, A.B. Petersen and C. Wittig, J. Chem. Phys. 65 (1976) 1872.
[6] R.J. Donovan and D. Husain, Trans. Faraday Soc. 62 (1966) 2643.
[7] T.W. Broadbent and A.B. Callear, J. Chem. Soc. Faraday II 68 (1972) 1367;
A. Gelb, R. Kapral and G. Burns, J. Chem. Phys. 59 (1973) 2980.

Volume 53, number 1 CHEMICAL PHYSICS LETTERS 1 January 1978

PHOTODISSOCIATION OF ALKYL BROMIDES

W.L. EBENSTEIN, J.R. WIESENFELD [‡] and G.L. WOLK
Department of Chemistry, Cornell University, Ithaca, New York 14853, USA

Received 1 September 1977

The branching ratios for the production of Br($4\,^2P_{1/2}$) and Br($4\,^2P_{3/2}$) following the broadband flash photolysis of the alkyl bromides, CH_3Br and C_2H_5Br, and the perfluorinated molecules, CF_3Br, C_2F_5Br and n-C_3F_7Br, have been determined using time-resolved atomic absorption spectroscopy. The production of electronically excited bromine atoms is shown to be inefficient in the case of the alkyl bromides while the perfluorinated molecules yield decreasing amounts of Br($4\,^2P_{1/2}$) as the molecular complexity increases, i.e., $CF_3Br > C_2F_5Br > C_3F_7Br$. It is also shown that the hydrogenated bromides deactivate electronically excited atoms almost two orders of magnitude faster than do the perfluorinated bromides.

1. Introduction

The production of electronically excited atoms during the photodissociation of small molecules has received much attention in recent years, with special emphasis on the photolysis of the alkyl iodides and their perfluorinated analogs [1–4]. The alkyl iodide experiments were stimulated in part by the observation [5] of laser action on the magnetic-dipole allowed transition,

$$I(5\,^2P_{1/2}) \rightarrow I(5\,^2P_{3/2}) + h\nu \ (\lambda = 1315 \text{ nm})$$

and the need to elucidate the mechanism of excited atom production during photolysis. The results of these investigations have led to a qualitative theory [4] regarding the effect of the parent molecule structure on the yields of the electronically excited species. The theory relates the observed correlation between alkyl group structure and the relative production of excited state atoms by using simple symmetry arguments which take into account the role of spin–orbit coupling in the photodissociative state [6].

The purpose of this investigation then is to test the theory and to determine the utility of various alkyl bromides as sources for the analogous bromine atom laser [7],

$$Br(4\,^2P_{1/2}) \rightarrow Br(4\,^2P_{3/2}) + h\nu \ (\lambda = 2713 \text{ nm}).$$

As the kinetics of Br($4\,^2P_{1/2}$) (hereafter Br*) following flash photolysis of the parent molecule are of importance in the Br* laser and in systems utilizing alkyl bromides as sources of ground or excited state bromine atoms, we have also measured rates of deactivation of Br* by the parent molecules and propose possible mechanisms for these processes.

2. Experimental

The apparatus utilized in these experiments has been described previously [3,4,8]. A dilute solution of the alkyl bromide (typically $1-50 \times 10^{-3}$ torr) in an argon buffer ($P_{\text{total}} \approx 20$ or 30 torr for perfluorinated species, 60 torr for alkyl bromides) was exposed to a light pulse from a Kr-filled flashlamp ($t_{1/2} \approx 10\ \mu s$, $E = 100$ J). Thermalization of species in the quartz reaction vessel was insured by the great excess of argon buffer gas. The temporal profiles of $[Br^*]_t$ or $[Br]_t$ ($Br \equiv Br(4\,^2P_{3/2})$) after the flash were monitored by observing the attenuation of atomic resonance radiation at 154.1 nm ($5\,^4P_{3/2} \leftarrow 4\,^2P_{3/2}$) or 153.2 nm ($5\,^2P_{1/2} \leftarrow 4\,^2P_{1/2}$). The resonance transitions were excited in a continuously operating, microwave-powered electrodeless discharge through a 10% Br_2–Ar mixture ($P_{\text{total}} = 0.2$ torr).

[‡] Camille and Henry Dreyfus Teacher–Scholar.

The transient absorption signal was monitored by employing an EMI solar blind photomultiplier tube and digitized with a Biomation 802 transient recorder. Typically 16–64 runs were averaged in order to enhance the signal.

Gases in the reaction vessel were swept out between individual kinetic runs. CF_3Br, C_2F_5Br, and n-C_3F_7Br (PCR, Inc.) were first degassed and then purified by repeated distillations. CF_3Br was distilled from a 40% pentane/60% ethanol slush (138 K) to liquid N_2, C_2F_5Br was distilled from a toluene slush (178 K) to liquid N_2, and C_3F_7Br was distilled from an acetone slush (187 K) to liquid N_2. CH_3Br (99.5%, Matheson) and C_2H_5Br (Fisher Certified) were similarly degassed and distilled, CH_3Br from an acetone slush to liquid N_2, and C_2H_5Br from a chlorobenzene slush (228 K) to liquid N_2. Research grade H_2 (Matheson) was used without further purification. Ultra high purity argon (Matheson) was passed over a molecular sieve at 193 K immediately before use.

All mixtures were prepared on a Hg-free glass vacuum line which was evacuable to $\approx 10^{-6}$ torr. The composition of the gas mixture in the reaction vessel was determined using calibrated floating ball rotameters. Pressures were measured with a glass Bourdon gauge and standard test gauges.

3. Results

The removal of Br* was monitored using the resonance transition at 153.2 nm, the absorption signal being related to $[Br^*]_t$ by

$$\ln(I_0/I_t) = (\epsilon l [Br^*]_t)^\gamma, \qquad (1)$$

where the constants have been previously described [9]. The intensity of the radiation before the flash, I_0, was measured using the pretrigger record feature of the transient recorder. An experimental value of γ (typically 0.60–0.90) was determined over the range of observed absorption by measuring the absorbance of Br* at time $t = 0$ ($\approx$20 μs after the flash) while varying the pressure of the source gas. The pseudo-first order rate constant, k, derived from the transient absorption measurements ($[Q] > [Br^*]_t$) may be related to the bimolecular rate constant for deactivation, k_Q, by

$$k = k_Q[Q] + K,$$

where K represents removal of Br* by spontaneous emission, diffusion to the walls of the reaction vessel and quenching by impurities in the samples of alkyl bromides or argon buffer. A plot of k versus [Q] ([Q] = alkyl bromide pressure) gives a straight line of slope k_Q.

Table 1

Source	Φ	p^*	$10^{13}\,k$ (cm^3 molec^{-1} s^{-1})
CF_3Br	2.0	0.66 ± 0.07	1.20 ± 0.2 0.5 [a]
C_2F_5Br	0.9	0.48 ± 0.02	2.7 ± 0.4
n-C_3F_7Br	<0.1	<0.10	3.8 ± 0.3
CH_3Br	0.2	0.15 ± 0.12	77 ± 7
C_2H_5Br	<0.1	<0.10	121 ± 8

[a] Ref. [11].

The results of these kinetic experiments are presented in table 1 and fig. 1. They clearly indicate that the hydrogenated bromides are $\approx$100 times more efficient at deactivating Br* than are the perfluorinated bromides.

The branching ratios ($\Phi = [Br^*]_0/[Br]_0$) and fractional yields of Br* ($p^* = [Br^*]_0/([Br^*]_0 + [Br]_0)$) were determined using the following technique. A given pressure of alkyl bromide was photolyzed in the absence of all gases other than the argon buffer (fig. 2a). The absorption measured immediately following the flash then represents $[Br]_0$, the concentration of ground state Br atoms produced photolytically.

The addition of an excess ($\approx$0.1 torr) of H_2 to the photolysis mixture described above results in the rapid ($t_{1/2} = (k_{H_2}[H_2])^{-1} \approx 10^{-5}$ s) relaxation of Br* produced in the flash. All of the Br* deactivated in this fashion relaxes to form ground state atoms; reactive processes play no role here, as formation of HBr + H from Br* + H_2 is 7 kcal/mole endothermic. Therefore the absorption immediately following the flash (fig. 2b) may be related to the total production of bromine atoms, $[Br^*]_0 + [Br]_0$.

This technique has been previously applied to the reaction of excited iodine atoms with HBr and DBr [8]. The kinetic equations governing the disappearance of Br* and the appearance of Br have been thoroughly described in ref. [8] and will not be repeated here. In the absence of a reactive species, the equations for Φ and p^* are simply:

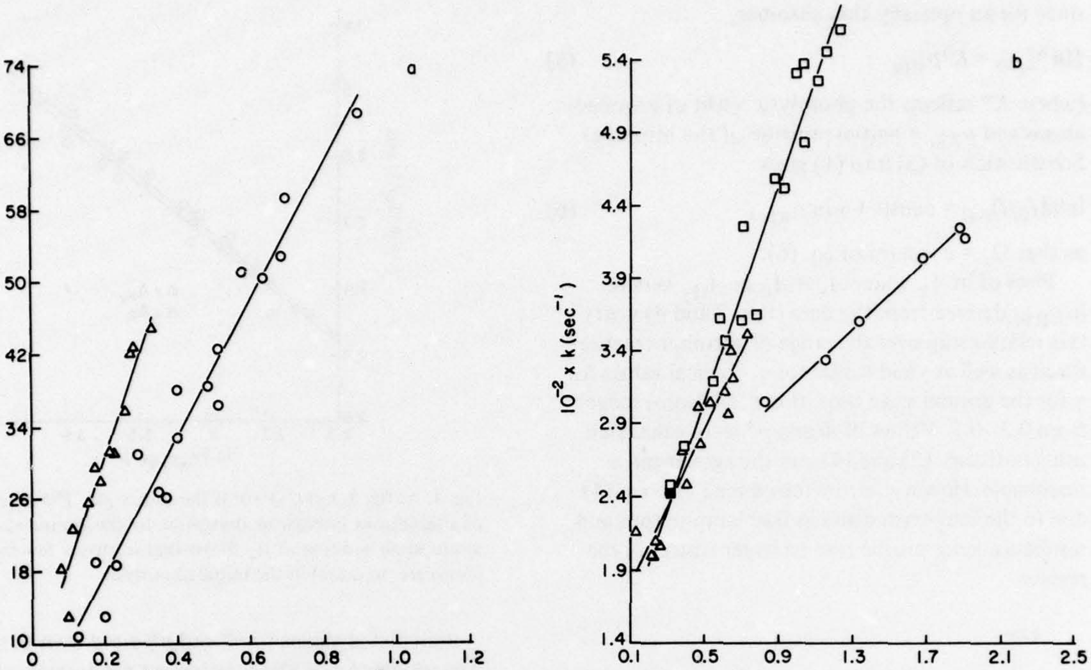

Fig. 1. Plots of pseudo-first-order rate coefficients for removal of $Br(4\,^2P_{1/2})$ versus density of deactivating gas. (a) ○ CH_3Br, △ C_2H_5Br; (b) ○ CF_3Br, △ C_2F_5Br, □ C_3F_7Br. *For the sake of clarity, only a representative sample of data points is shown.*

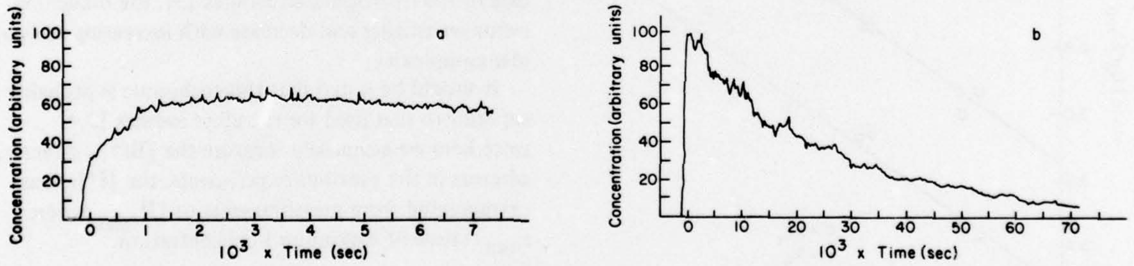

Fig. 2. Temporal profiles of $[Br(4\,^2P_{1/2})]$ following photolysis of 0.017 torr CF_3Br in 30 torr Ar. (a) $p_{H_2} = 0$, (b) $p_{H_2} = 0.22$ torr. Traces represent an average of 32 kinetic runs.

$$\Phi = (A_{H_2}^{\gamma^{-1}} - A_0^{\gamma^{-1}})/A_0^{\gamma^{-1}}, \tag{2}$$

$$p^* = (A_{H_2}^{\gamma^{-1}} - A_0^{\gamma^{-1}})/A_{H_2}^{\gamma^{-1}}, \tag{3}$$

where $A_{H_2} = (\epsilon l[Br]_0 + \epsilon l[Br^*]_0)^\gamma$, the absorbance measured in the presence of H_2 and $A_0 = (\epsilon l[Br]_0)^\gamma$, the initial absorbance measured in the absence of H_2.

Alternatively Φ may be written as

$$\Phi = \frac{\exp(\Omega_{H_2}/\gamma) - \exp(\Omega_0/\gamma)}{\exp(\Omega_0/\gamma)}, \tag{4}$$

since for an optically thin absorber,

$$[\mathrm{Br}^*]_{t=0} = K^* p_{\mathrm{RBr}} \tag{5}$$

(where K^* reflects the photolytic yield of bromine atoms and p_{RBr} = partial pressure of the bromide). Substitution of (5) into (1) gives

$$\ln\ln(I_0/I)_{t=0} = \text{const.} + \gamma \ln p_{\mathrm{RBr}}, \tag{6}$$

so that Ω_x = constant of eq. (6).

Plots of $\ln A_x$ where $A_x = A_0$ or A_{H_2} versus $\ln p_{\mathrm{RBr}}$ derived from the data (figs. 3 and 4) verify this relationship over the range of absorbances measured as well as yield values for γ. Typical values for γ for the ground state transition (154.1 nm) range from 0.3–0.5. Values of Φ and p^* were calculated using both eqs. (2) and (4) and the agreement is reasonable. However errors introduced into eq. (4) due to the long-term drifts in flashlamp output and resonance lamp profile lead to larger scatter in the results.

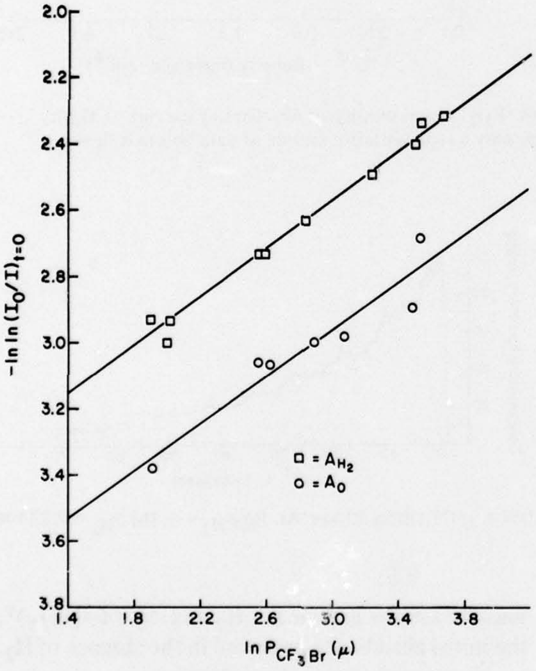

Fig. 3. Plot of $-\ln\ln(I_0/I)_0$ versus $\ln p_{CF_3Br}$ demonstrating the validity of eqs. (4) and (6). The increased absorption observed when H_2 is added to the reaction mixture represents the deactivation of $\mathrm{Br}(4\,^2P_{1/2})$ to $\mathrm{Br}(4\,^2P_{3/2})$. Only a sample of data points is shown here.

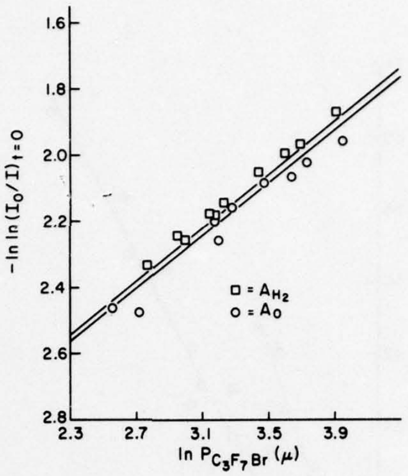

Fig. 4. As fig. 3, but C_3F_7Br is the source gas. The absence of a significant increase in absorption by the ground state atoms upon addition of H_2 shows that relatively few excited atoms are produced in the initial photolysis.

Calculated values for Φ and p^* are shown in table 1. The results clearly show decreased production of Br* versus Br, as one proceeds through the homologous series,

$$CF_3Br > C_2F_5Br > C_3F_7Br.$$

In the case of the hydrogenated bromides, as in the case of the hydrogenated iodides [3], the branching ratios are smaller and decrease with increasing molecular complexity.

It should be noted that this technique is probably superior to that used for the alkyl iodides [3,4] since here we essentially measure the $[\mathrm{Br}^*]_0$ directly, whereas in the previous experiments, the $[\mathrm{I}^*]_0$ was extrapolated from measurements of $[\mathrm{I}]_{t_{\max}}$ where $t_{\max}$ = time of maximum I concentration.

4. Discussion

As may be seen from table 1, the alkyl bromides are relatively inefficient photolytic sources of Br*, the only molecules capable of producing laser action (threshold requires $\Phi > 0.5$) being CF_3Br and C_2F_5Br. In addition the branching ratios are substantially smaller than those observed for RI [3,4]. This observation may be viewed in the context of the earlier theory devised to explain the dependence of branching ratio on source molecule structure of the alkyl iodides [4]. The production of excited bromine atoms will result following direct population of the lowest excited A_1^* state of the alkyl bromide

$$\mathrm{RBr}(A_1) \xrightarrow{h\nu} \mathrm{RBr}(A_1^*),$$

$$\mathrm{RBr}(A_1^*) \rightarrow \mathrm{R}\cdot + \mathrm{Br}(4\,^2P_{1/2}).$$

The lower yields of excited bromine atoms may then simply be explained in terms of two reinforcing phenomena. Firstly, the spin–orbit splitting in the alkyl bromides will be inherently smaller than in the iodides due to the lower atomic number of bromine. Secondly, the electronegativity of bromine is higher than that of iodine, thereby resulting in the energetic stabilization of zwitterionic valence structures [10] of the form R^+Br^-, where $Br^-(^1S_0)$ contributes nothing to the magnitude of the spin–orbit coupling in the molecular excited state. Thus, the A_1^* state cannot accurately be discussed in terms of strong spin–orbit coupling and the correlation between this molecular state and R + Br*, which is valid only in the case of strong coupling, is relatively poor. The yield of electronically excited bromine atoms in the photolysis of alkyl bromides is relatively low when compared to the corresponding observations in iodine.

It should be further noted that the perfluorinated alkyl bromides display lower branching ratios for the formation of Br* as the molecular complexity increases in apparent contradiction to the trend observed in the analogous iodides where the values of Φ are $CF_3I < C_2F_5I < n\text{-}C_3F_7I$ [3]. No simple explanation of this observation may be extracted from the qualitative theory. The data do suggest, however, that for alkyl bromides for which the alkyl radicals display very similar ionization potentials (and hence would show comparable contributions of zwitterionic structure), secondary structural effects will play a significant role in determining the branching ratio.

The alkyl bromides are clearly seen to be far more efficient in deactivating Br* than are the perfluorinated molecules. This is presumably due to the relatively close resonance between the magnitude of the electronic quantum in bromine, 3686 cm^{-1}, and the C–H stretch, ca. 3000 cm^{-1}, which can significantly enhance the efficiency of electronic-vibrational energy transfer [8]. No such close resonance occurs in the case of the perfluorinated molecules. Alternatively, the deactivation of Br* may take place via an atom transfer reaction,

$$\mathrm{Br}_a^* + \mathrm{RBr}_b \rightarrow \mathrm{RBr}_a + \mathrm{Br}_b,$$

although it is difficult to understand why such a process would be over one order of magnitude more efficient for the hydrogenous bromides.

References

[1] R.J. Donovan, F.G.M. Hathorn and D. Husain, Trans. Faraday Soc. 64 (1968) 3192.

[2] S.J. Riley and K.R. Wilson, Discussions Faraday Soc. 53 (1972) 132.

[3] T. Donahue and J.R. Wiesenfeld, Chem. Phys. Letters 33 (1975) 176.

[4] T. Donahue and J.R. Wiesenfeld, J. Chem. Phys. 63 (1975) 3130.

[5] K. Hohla and K.L. Kompa, in: Handbook of chemical lasers, eds. R.W.F. Gross and J.F. Bott (Wiley, New York, 1976) p. 667.

[6] A.B. Nikolskii, Opt. Spectry. 29 (1970) 560.

[7] J.D. Campbell and J.V.V. Kasper, Chem. Phys. Letters 10 (1971) 436.

[8] J.R. Wiesenfeld and G.L. Wolk, J. Chem. Phys. 65 (1976) 1506.

[9] P.D. Foo, T. Lohman, J. Podolske and J.R. Wiesenfeld, J. Phys. Chem. 79 (1975) 414.

[10] W.G. Dauben, L. Salem and N.J. Turro, Accounts Chem. Res. 8 (1975) 41.

[11] R.J. Donovan and D. Husain, Trans. Faraday Soc. 62 (1966) 2643.

SECURITY CLASSIFICATION OF THIS PAGE (When Data Entered)

REPORT DOCUMENTATION PAGE

READ INSTRUCTIONS
BEFORE COMPLETING FORM

1. REPORT NUMBER

2. GOVT ACCESSION NO.

3. RECIPIEN~~T'S CATALOG N~~UMBER

summary

4. TITLE (and Subtitle)

6

Dynamics of the Chemistry of Electronically Excited Atoms in Defined Quantum States.

5. TYPE OF REPORT & PERIOD COVERED

9

Annual Report ~~4/1/77 - 3/31/78~~

1 Apr 77 - 31 Mar 78,

6. PERFORMING ~~ORG. REPORT NUMBER~~

7. AUTHOR(s)

10

John

~~J.~~ R. Wiesenfeld

8. CONTRACT OR GRANT NUMBER(s)

15

N00014-75-C-0828

9. PERFORMING ORGANIZATION NAME AND ADDRESS

Cornell University
Ithaca, New York 14853

10. PROGRAM ELEMENT, PROJECT, TASK AREA & WORK UNIT NUMBERS

NR 394-010

11. CONTROLLING OFFICE NAME AND ADDRESS

Office of Naval Research
Physics Program Office
Arlington, Virginia 22217

12. ~~REPORT DATE~~

11

1 May 1978

13. ~~NUMBER~~ OF PAGES

12

25 p.

14. MONITORING AGENCY NAME & ADDRESS (if different from Controlling Office)

15. SECURITY CLASS. (of this report)

Unclassified

15a. DECLASSIFICATION/DOWNGRADING SCHEDULE

16. DISTRIBUTION STATEMENT (of this Report)

Approved for public release; distribution unlimited

17. DISTRIBUTION STATEMENT (of the abstract entered in Block 20, if different from Report)

18. SUPPLEMENTARY NOTES

19. KEY WORDS (Continue on reverse side if necessary and identify by block number)

Chemical Lasers
Chemical Reactions
Photochemistry
Photolysis

20. ABSTRACT (Continue on reverse side if necessary and identify by block number)

The photodissociation of alkyl bromides and their perfluorinated analogues has been investigated. The quantum yield of $Br(4^2P_{1/2})$ production is <0.10 except for CF_3Br and C_2F_5Br. The continuous absorption spectrum of Br_2 has been studied and the relative contributions for absorption into the $B^3\pi_{0^+u}$, $A^3\pi_{1u}$ and $^1\pi_{1u}$ states assessed using Laser Induced Photodissociation Spectroscopy. The deactivation of $I(5^2P_{1/2})$ with Br_2 has been shown to proceed primarily *via* adiabatic reaction to form $Br(4^2P_{1/2})$, a process which
(over)

DD FORM 1 JAN 73 1473 EDITION OF 1 NOV 65 IS OBSOLETE
S/N 0102-LF-014-6601

SECURITY CLASSIFICATION OF THIS PAGE (When Data Entered)

098 550

20. Continued

should be useful for pumping a bromine atom electronic transition laser in the infra-red.

IED

-78